Proc. Natl. Acad. Sci. USA
Vol. 85, pp. 5956–5960, August 1988
Cell Biology

The role of lipids in *Plasmodium falciparum* invasion of erythrocytes: A coordinated biochemical and microscopic analysis

(parasite–host membrane junctions/parasitophorous vacuole membrane)

ROSS B. MIKKELSEN*, MARKUS KAMBER*, KALYAN S. WADWA†, PECK-SUN LIN*, AND RUPERT SCHMIDT-ULLRICH*

Radiobiology Division, Department of Radiation Oncology, New England Medical Center Hospitals, Boston, MA 02111

Communicated by William Trager, April 11, 1988 (received for review January 8, 1988)

ABSTRACT **The role of lipids in *Plasmodium falciparum* invasion of erythrocytes was investigated by biochemical and fluorescent microscopic analysis. Metabolic incorporation of radioactive oleate or palmitate and fractionation of radiolabeled phospholipids by thin-layer chromatography revealed no difference in the major phospholipid classes of schizonts and early ring forms after merozoite invasion. Fluorescent anthroyloxy derivatives of oleate and palmitate were also metabolically incorporated into parasite phospholipids. By microscopic analysis, the fluorescent phospholipids were seen localized in the plasma membrane and, within the merozoite, concentrated near the apical end. During invasion fluorescent phospholipid appeared to be injected from the apical end of the merozoite into the host membrane, both within and outside the parasite–host membrane junctions. After invasion fluorescent lipid was only found in the parasite plasma membrane and/or parasitophorous vacuole membrane. Parallel experiments with a fluorescent cholesterol derivative, incorporated into parasite membranes by exchange, revealed neither heterogeneous distribution of label within the parasite nor evidence for cholesterol transfer from merozoite to host cell membrane. Results suggest that during invasion no major covalent alteration of parasite lipids, such as lysophospholipid formation, occurs. However, invasion and formation of the parasitophorous vacuolar membrane apparently involves insertion of parasite phospholipids into the host membrane.**

A highly efficient invasion of erythrocytes by *Plasmodium* merozoites is essential for rapid parasite multiplication. Early kinematographic and EM studies of merozoite invasion (1–3) showed the complex structural events in this intricate cellular interaction. More recent studies show the initial interaction between *Plasmodium falciparum* (*Pf*) merozoite and erythrocyte to be mediated by specific receptors on both cells (4–8). The requirement for the merozoite to attach with its apical end before successful invasion (2, 9) and the observation that the rhoptry–microneme complex of the merozoite extends to the apical end (2, 9, 10) suggest the rhoptries contain material released by the parasite upon invasion. Recently, fixation of merozoites with tannic acid has permitted EM visualization of membranous whorls associated with the rhoptries near the apical end of *Pf* merozoites. These whorls most likely represent multilayered lipid and lipid/protein structures (10, 11). Immunochemical and biochemical studies have localized in *Pf* merozoite rhoptries a M_r 140,000 *Pf* protein (*Pf*140) that coprecipitates with a M_r 155,000 protein (*Pf*155), which also may be stored in the rhoptry–microneme complex (12). What either protein does during invasion is unclear, but a *Pf*155 antigen was found associated with the inner surface of membranes of freshly invaded erythrocytes (13).

The publication costs of this article were defrayed in part by page charge payment. This article must therefore be hereby marked "*advertisement*" in accordance with 18 U.S.C. §1734 solely to indicate this fact.

During invasion the host cell membrane rapidly expands around the parasite to form the parasitophorous vacuole membrane (PVM). How this expansion occurs is unknown, but it may involve the insertion of parasite lipids into the host cell membrane during invasion. Freeze–fracture studies (14–16) of the PVM show relative depletion of intramembranous particles in the outer leaflet of the PVM, suggesting a relative lipid content higher than normally seen in erythrocyte membranes.

We directly examined the fate of lipids during *Pf* invasion. *Plasmodia* are incapable of *de novo* fatty acid or cholesterol synthesis and get these membrane components from their host (17, 18). We used this feature of parasite metabolism to label *Pf* phospholipids with radioactive and fluorescent fatty acids and to introduce by exchange a fluorescent derivative of cholesterol into parasite membranes. This experimental approach permitted biochemical and image analyses, using digitized video-intensified fluorescence microscopy, of the role of lipids in *Pf* invasion of erythrocytes.

MATERIAL AND METHODS

Reagents. Reagents were obtained from the following suppliers: Lecithin, phospholipid standards, and bovine serum albumin from Sigma; Percoll from Pharmacia; silica gel TLC plates from Brinkmann Instruments; 12-(9-anthroyloxy)-oleic acid (12-AOle), 2-(9-anthroyloxy)-palmitic acid (2-APam), and 25-[7-nitrobenz-2-oxa-1,3 diazol-4-yl]-27-norcholesterol (NBD-norcholesterol) from Molecular Probes (Eugene, OR); [9,10-^{3}H(N)]oleic and palmitic acids from New England Nuclear. Human serum and erythrocytes, washed twice, from O type rhesus factor-positive donors were prepared in our laboratory.

***Pf* Culture.** The cloned *Pf* strain, T9/96 from Thailand, was maintained, essentially as described by Trager and Jensen (19), at 5% hematocrit in T25 or T75 closed tissue culture flasks equilibrated with $O_2/CO_2/N_2$ (5/5/90, vol/vol). The RPMI 1640 (GIBCO) culture medium supplemented with 10% human serum/3.5 mM $NaHCO_3$/10 mM glucose/13 mM *N*-Tris[hydroxymethyl]methyl-2-aminoethanesulfonic acid/0.4 mM hypoxanthine/2 mM glutamine/gentamycin at 2 μg/ml was changed daily. Synchronized cultures were obtained by collection of schizont-infected erythrocytes atop isotonic Percoll, 64–72%, once per week essentially as reported (20).

Abbreviations: *Pf*, *Plasmodium falciparum*; mAb, monoclonal antibody; PVM, parasitophorous vacuole membrane; 12-AOle, 12-(9-anthroyloxy)-oleic acid; 2-APam, 2-(9-anthroyloxy)-palmitic acid; NBD-norcholesterol, 25-[7-nitrobenz-2 oxa-1,3-diazol-4-yl]-27-norcholesterol.

*Permanent address: Department of Radiation Oncology, Medical College of Virginia, Richmond, VA 23298.
†Permanent address: Dermatology Department, Tufts School of Medicine, Boston, MA 02111.

Metabolic Labeling. For metabolic labeling, synchronized *Pf* cultures were exposed to radioactive or fluorescent lipids during the late trophozoite/schizont stages for periods of 5–16 hr. *Pf*-infected erythrocytes were incubated with [^{3}H]oleic acid at 0.37 μg/ml (3×10^6 cpm/ml) under standard culture conditions. After labeling, the parasites were collected by centrifugation at 500 × *g* for 10 min and washed twice in RPMI 1640/1% bovine serum albumin. Identical labeling procedures were used with 12-AOle or 2-APam at 50–100 μg/ml. Microscopic analysis revealed identical labeling distributions at either 5 or 16 hr of incubation.

NBD-norcholesterol was incorporated by exchange using egg lecithin/NBD-norcholesterol liposomes prepared at a 1:1 molar ratio. The liposomes were prepared aseptically and added to cultures for 16 hr at a final NBD-norcholesterol concentration of 200 μg/ml.

For biochemical lipid analysis, metabolically labeled schizonts were purified to a parasitemia of >80% atop Percoll gradients (20). Ring-infected erythrocytes were produced by diluting purified schizonts with fresh erythrocytes to a parasitemia of ≈30%. Within several hours ring-stage parasites appeared at a parasitemia of 20% and 35%. Before lipid extraction, the remaining schizonts were quantitatively removed by use of Percoll gradients.

Lipid Analysis. Purified schizont- or ring-stage infected erythrocytes were extracted twice in a 20-fold volume of chloroform/methanol (2:1, vol/vol) (21). The combined extracts were dried under N_2 and redissolved in chloroform/methanol. Final volumes were adjusted to contain lipids from 10^6 parasitized and 10^8 normal erythrocytes per μl of extract.

TLC chromatograms were developed in chloroform/methanol/acetic acid/0.1 M sodium borate (75:45:12:4.5, vol/vol), a solvent system that permits resolution of the major phospholipid fractions and their lysophospholipid derivatives (17). The 15-cm-long lanes containing the parasite lipids labeled with ^{3}H-containing fatty acids and standards were collected in 30 fractions and transferred into scintillation vials holding 3 ml of Aquasol-2 for counting. Reference lipids were visualized with iodine vapor.

Anthroyloxy-labeled lipids were visualized using a UV mineral light and photographed. Densitometric scans of the negatives were used to measure the relative amounts of lipids.

Purification of Human Monoclonal Antibodies. Two Epstein–Barr virus-transformed human B-lymphocyte lines, SS2F4 and SS2D2 (22), secreting monoclonal antibodies (mAbs) against *Pf*195 were fused (23) with the HAT (hypoxanthine/aminopterin/thymidine)-sensitive, ouabain-resistant lymphoblastoid cell line KR-4 (24) for increased stability (M.K., unpublished results). The mAbs were purified from spent culture supernatants by affinity chromatography on goat anti-human IgG coupled to Sepharose 4B. After elution with 0.1 M glycine/HCl, pH 2.5, the mAbs were neutralized with 1 M Tris, pH 8.0, dialyzed against phosphate-buffered saline, concentrated by ultrafiltration over PX-10 membranes (Amicon), and filtered (0.22-μm pore size; Millipore). Protein concentrations were determined by absorption at 280 nm, with 1.4 unit at A_{280} corresponding to 1 mg/ml.

Effect of mAb on Reinvasion. Synchronized parasites were labeled with 12-AOle at 100 μg/ml for 5 hr before reinvasion. mAb was added to a final concentration of 100 μg/ml 2 hr before the time of expected reinvasion and was present for a total of 4 hr until most schizont-infected erythrocytes had lysed. Cells were fixed and examined microscopically.

Microscopic Analysis. Parasitized erythrocytes labeled with 12-AOle or 2-APam were examined at 30-min intervals with Giemsa staining to determine peak time of merozoite release. At this time cells were washed once with culture medium and examined by fluorescence microscopy, either live or after fixation with 0.2% glutaraldehyde in phosphate-buffered saline.

A Zeiss 100× oil-immersion Neofluor (n.a. 1.3) objective lens was used with a Zeiss Universal epiillumination microscope and a 75 W Xenon arc. Excitation frequencies for 12-AOle and NBD-norcholesterol were selected with band-pass filters, 380 nm (10 nm, 0.5 bandwidth) and 470 nm (12 nm, 0.5 bandwidth), respectively. Emission was monitored with long-pass filters at 410 nm and 500 nm for 12-AOle and NBD-norcholesterol, respectively.

Images were obtained with a Dage (Michigan City, IN) model MTI66 silicone-intensified target camera and digitized using a Digital Equipment Microvax II microcomputer and Imaging Technology video boards (IP-512 series). To increase the signal-to-noise ratio, eight video frames were averaged for each image. The effective magnification of some images was increased at the display monitor by the computer software.

RESULTS

Distributions of metabolically incorporated [^{3}H]oleic or [^{3}H]palmitic acid into the four major phospholipid fractions were found similar in schizonts and freshly invaded ring-stage parasites freed of schizonts by Percoll fractionation. Results for oleic acid are shown in Table 1, but similar results were obtained with palmitic acid. For both precursors, ≥75% of the label was incorporated into phospholipid with the balance comigrating with the neutral lipid fraction, e.g., triglycerides (17) and nonincorporated fatty acid. When corrected for cell number, uninfected cells incorporated only 0.2–0.5% of the label found for parasitized erythrocytes. This >100-fold metabolic use of ^{3}H-labeled fatty acids by infected cells precludes any significant contribution, under our experimental conditions, from the lipids of uninfected erythrocytes to the labeling results. There was no indication of lysophospholipid formation during the 2- to 3-hr period in which merozoites were released and early ring-stage parasites appeared.

The above results cannot be strictly compared with previous studies on palmitate/oleate incorporation into *Pf* lipids (17) because labeling conditions were substantially different (e.g., incubation time in ref. 17 was 3 hr versus 16 hr in our work). The relative amounts of phosphatidylcholine and phosphatidylethanolamine labeled with oleate in the two studies differ, probably reflecting the longer incubation times in the present study and conversion of phosphatidylethanolamine into phosphatidylcholine (17). However, the incorpo-

Table 1. [^{3}H]Oleate incorporation into *Pf*/human erythrocyte phospholipids

Parasite stage	Phospholipids, %		
	Phosphatidylcholine	Phosphatidylserine/inositol	Phosphatidylethanolamine
Schizonts*	45.6 ± 4.7	8.2 ± 1.9	16.9 ± 2.6
Rings†	47.1 ± 3.6	9.4 ± 2.0	20.1 ± 4.3
Noninfected erythrocytes‡	69.6 ± 0.5	1.9 ± 0.1	17.1 ± 0.9

*Results represent the average of five experiments with cell populations of 50–60% schizonts.
†Results represent the average from eight experiments with cell populations of 20–30% ring-stage parasites.
‡Results averaged for two cell preparations.

ration rates for oleate into phosphatidylcholine are similar (15 versus 30 nmol per 10^{10} cells per hr in ref. 17).

Quantitative fluorescence analysis of TLC plates of fractionated 12-AOle-labeled phospholipids indicated that these derivatives were used with about the same efficiency as the [^{3}H]oleate/[^{3}H]palmitate with >85% of the label found in the phospholipid fraction. Thus, the microscopic analysis described below follows the fate of metabolically labeled phospholipids rather than free fatty acids.

In determining the labeling conditions for 12-AOle we found that 12-AOle at 50–100 μg per ml yielded excellent image quality with minimum toxicity. However, incubation of infected erythrocytes for 16 hr with 12-AOle at 100 μg/ml, caused a 3- to 4-hr lag in peak invasion time compared with nonlabeled controls. If infected cells were incubated during the last 5 hr of schizogony, no apparent delay in merozoite release was seen. At 200 μg/ml, reinvasion was inhibited and a large number of free parasites were seen.

Fig. 1 shows representative parasites labeled with 12-AOle at 100 μg/ml for 16 hr; identical results were obtained with 2-APam. Variations in background and host-membrane fluorescence among the different images in Fig. 1 and subsequent figures are due, in part, to the autogain function of the video camera, which automatically adjusts gain, and thus background, to achieve maximal brightness. Because both photobleaching and parasite movement (especially merozoites) presented focusing problems, we show two images of each developmental stage of the parasite.

Fig. 1 *A* and *B* shows a parasite in the late trophozoite/early schizont stage with extensive intracellular fluorescence. Segmenters (Fig. 1 *C* and *D*) exhibit discrete fluorescence localized to each merozoite. Comparing the relative size of the fluorescent area with merozoite size in the phase-contrast image suggests that the fluorescence is not uniformly distributed throughout the merozoite. This distribution is confirmed by the images of free merozoites (Fig. 1 *E–H*). A rim of fluorescence surrounds the parasite, but most fluorescent lipid is concentrated at one end of the merozoite. When parasites at the schizont stage are diluted at peak invasion time with unlabeled erythrocytes, the resulting early rings demonstrate, depending on the focal plane, a rim of fluorescence without any obvious intracellular concentration of fluorescent lipid (Fig. 1 *I–L*).

Video recording of the entire invasion process was not possible because of extensive photobleaching. However, using cultures fixed with glutaraldehyde during peak invasion time, many images of parasites during invasion have been captured. Fig. 2 *A* and *B* shows images of merozoites captured early in the invasion process; at this stage, the concentrated fluorescent lipid of the merozoite is invariably found at the invasion site. Fig. 2 *A* and *B* both show fluorescence spreading from the invasion site, suggesting that early in invasion, parasite phospholipid is injected into the host membrane both within and outside the parasite–host cell junction. Further into invasion, lipid appears to flow counter to the direction of the invading parasite, such that toward the end of invasion (Fig. 2*C*) fluorescent lipid no longer concentrates at the anterior end of the invading parasite but appears posterior. After invasion is completed and depending on cell orientation and focus, two concentric fluorescent rings are sometimes seen—possibly representing the parasite within the PVM (Fig. 2*D*). Projections of fluorescent lipid into the erythrocyte space are also commonly seen during and immediately after invasion (Fig. 2 *E* and *F*). The outer concentric ring, as well as these projections, may represent the PVM. Fluorescent labels specific for the PVM are required for any confirmation of this hypothesis.

Additional evidence for lipid transfer from parasite to host cell membrane comes from experiments in which the invasion process was interrupted by treatment with mAb against *Pf*195. This mAb inhibits *Pf* growth *in vitro*, presumably through its interaction with the merozoite *Pf*195 antigen (23). Incubation of synchronized cultures at the late schizont stage with mAb increased by 5- to 10-fold the free, as well as the attached but not invaded, merozoites compared with control cultures without mAb. Image analysis of 12-AOle-labeled

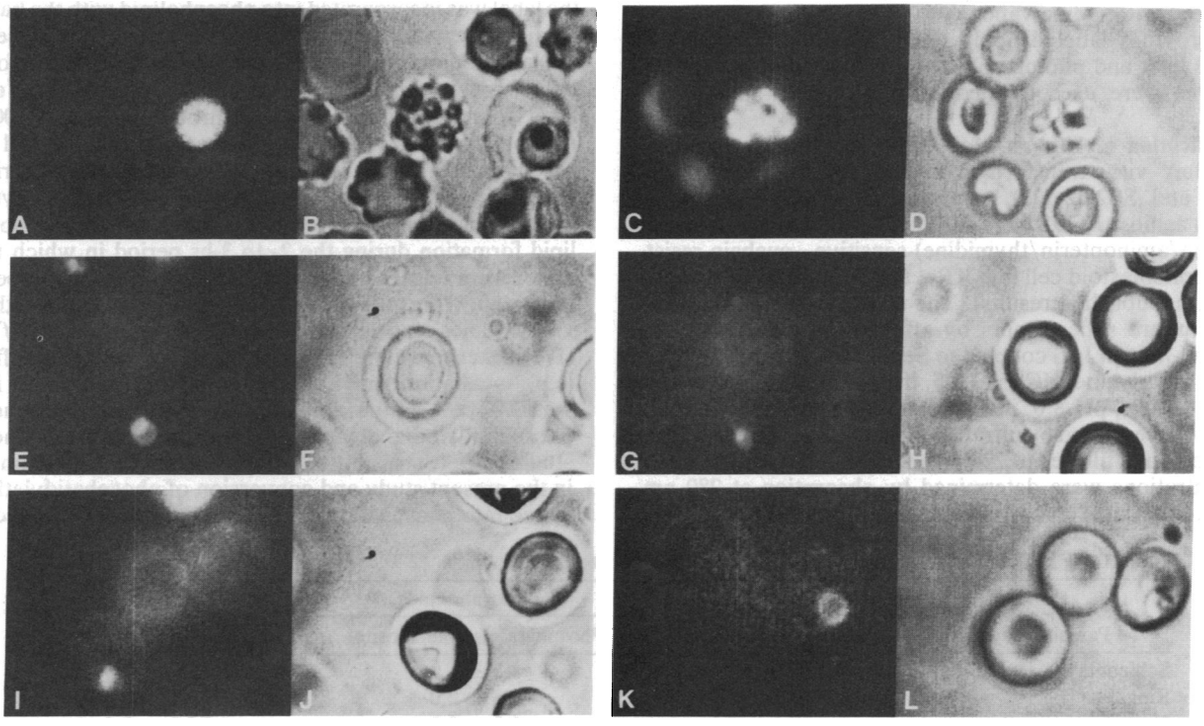

FIG. 1. Fluorescence and corresponding phase-contrast images of *Pf* at different developmental stages metabolically labeled with 12-AOle. (*A* and *B*) Schizont, (*C* and *D*) segmenter, (*E–H*) merozoite, and (*I–L*) postinvasion ring. Cells were viable and not fixed with glutaraldehyde. (×2000.)

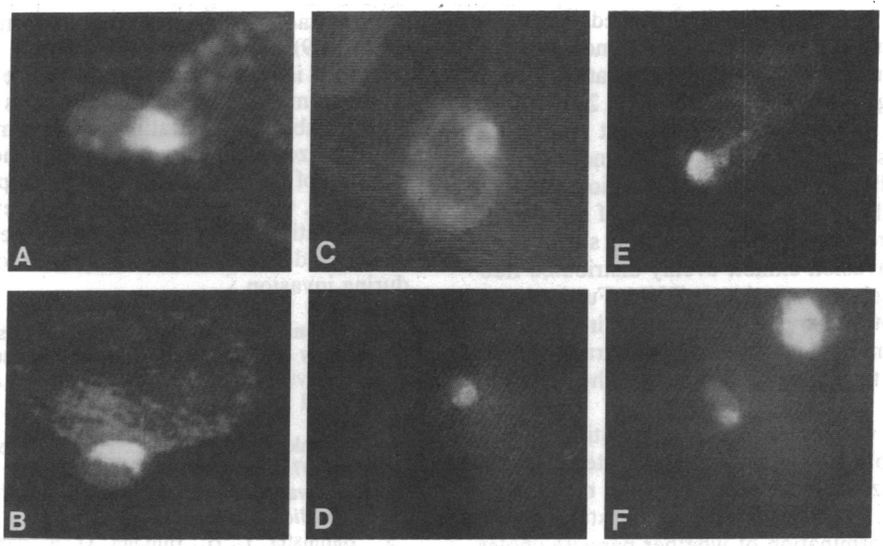

FIG. 2. Invasion of erythrocytes by 12-AOle-labeled *Pf*. Cells were fixed with 0.2% glutaraldehyde and examined microscopically. (*A*) ×7000, (*B*) ×3500, (*C*) ×2100, (*D–F*) ×1400. Differences in background fluorescence are from different gain settings for the video camera.

parasites incubated with mAb showed that free and attached mAb-treated merozoites lack the pronounced concentration of fluorescent lipid at the apical end (compare Fig. 3 with Fig. 1 *E* and *G* and Fig. 2 *A* and *B*). No evidence of lipid redistribution is found in attached merozoites treated with mAb.

We also examined the distribution of a fluorescent cholesterol derivative, NBD-norcholesterol, during erythrocytic *Pf* development. In all parasite stages examined, fluorescence is localized to the parasite plasma membrane (or PVM) and small subcellular vesicles. No concentration at the apical end of the merozoite is seen (Fig. 4).

DISCUSSION

By metabolic incorporation of ^{3}H-labeled fatty acids into phospholipids, we investigated whether covalent changes of parasite lipids are involved in invasion. No evidence for major alteration in phospholipid fractions or lysophospholipid formation was found. We cannot, however, rule out small transient changes. But lysophospholipids that act as fusogenic agents or help expand membrane surface area apparently do not have a prominent role in merozoite invasion of erythrocytes.

Metabolic labeling studies showed that >85% of 12-AOle is incorporated into phospholipids during *Pf* development. Microscopic analysis revealed that for trophozoites and schizonts most 12-AOle-labeled phospholipid was intracellular, which is not surprising because these stages of parasite development synthesize membranes for merozoite formation. With merozoites, incorporated 12-AOle was localized to the plasma membrane and concentrated at one end of the parasite—the apical end, we believe, because fluorescence is

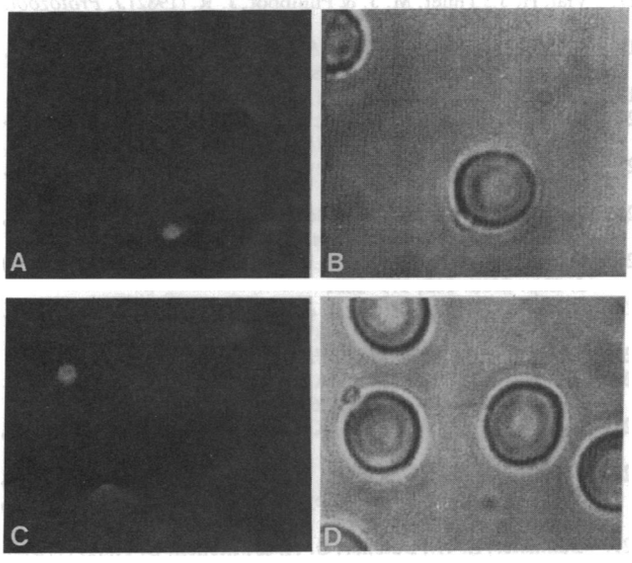

FIG. 3. The effect of mAb against *Pf*195 on the fluorescence image of 12-AOle-labeled merozoites. Cells were fixed with 0.2% glutaraldehyde. Figure shows paired fluorescence and phase-contrast images at ×1550.

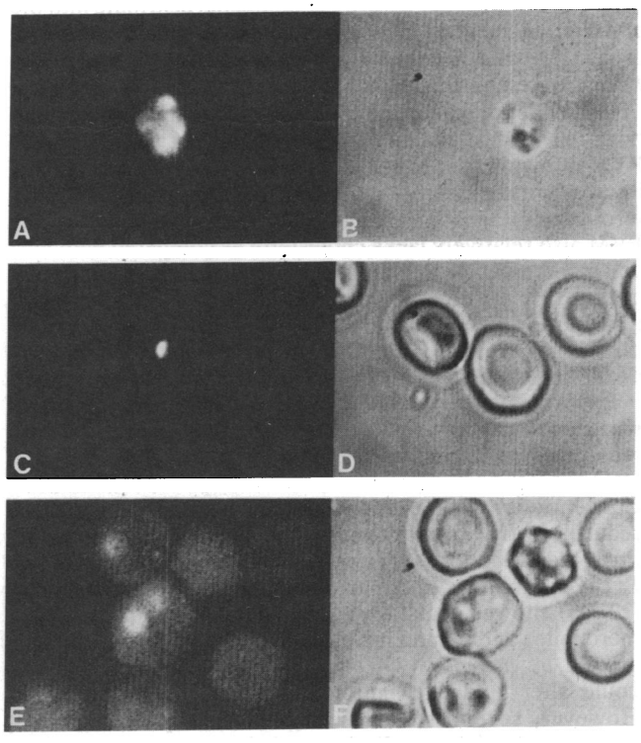

FIG. 4. *Pf* at different stages of development labeled with NBD-norcholesterol. Magnification was ×1550 for both fluorescence and corresponding phase-contrast images. (*A* and *B*) Segmenter, (*C* and *D*) merozoite, and (*E* and *F*) postinvasion ring.

found at the narrow end of the conical-shaped merozoite (compare Figs. 1 *E* and *G*, 2 *A* and *B*). Furthermore, images of merozoites early in invasion show concentrated fluorescence at the invading end of the parasite (Fig. 2 *A* and *B*). Although we cannot prove that the fluorescent lipid at the apical end associates with the rhoptries, absence of other membranous organelles in this merozoite region supports such a contention. This apical concentration of fluorescent lipid is transient, as are the rhoptries, in that ring stages of the parasite soon after invasion exhibit evenly distributed fluorescence within their plasma membrane/PVM. Furthermore, with merozoites captured by fixation during invasion, an injection of fluorescent lipid into the host membrane appears to be emanating from the point of attachment at the apical end of the merozoite.

In contrast to the nonhomogeneous distribution of fatty acid-labeled phospholipids, fluorescent cholesterol distributes within the merozoite more uniformly with no apparent apical concentration. Because NBD-norcholesterol photobleaches readily, determination of whether parasite cholesterol was also injected into the host membrane (as appears with phospholipids) was not possible.

The biochemical and microscopic studies suggest that during schizogony a pool of phospholipids is concentrated at the apical end, probably within the rhoptries. During invasion these lipids are transferred to the host membrane, where they may play a dominant role in modulating the membrane structure of host cells and in membrane expansion, thus facilitating invasion and formation of the PVM. The rapid transfer of phospholipids does not seem associated with covalent modification because the relative phospholipid composition of *Pf* appears unaltered after invasion. Although the implications of the following are not yet clear, some phospholipid distributes into the erythrocyte membrane—but outside the merozoite–erythrocyte junctions—as suggested by the halo-like fluorescence around the invading merozoite (Fig. 2 *A* and *B*). That parasite components distribute into the erythrocyte membrane is suggested by the data of Perlmann *et al.* (13), who demonstrated membrane association of the *Pf*155 protein in freshly invaded erythrocytes.

Our evidence for insertion of merozoite phospholipids into host cell membrane is compatible with EM studies on the PVM showing this membrane to be relatively depleted of intramembranous protein (14–16). Studies with the cholesterol-binding agent saponin support circumstantially that the PVM also relatively lacks cholesterol as compared with host cell membrane. At low saponin concentrations, in which the erythrocyte membrane is disrupted, the PVM appears intact (25) and the free parasites can use protein and nucleic acid precursors (26, 27). More drastic treatment with saponin does, however, strip off the PVM (28).

Experiments using mAb against the *Pf*195 component of merozoites support a role for *Plasmodium* membrane lipid redistribution during invasion. Many merozoites, free and attached to host cells, were seen after mAb treatment. Concentration of fluorescent lipid in the apical end was much reduced in free merozoites, and in attached merozoites no lipid redistribution was seen. These results suggest that *Pf*195 participates in the invasion process. Previous studies (22, 23) showed that *Pf*195 is localized to the periphery of merozoites and human mAb against *Pf*195 inhibited parasite growth *in vitro*. By what mechanism mAb against *Pf*195 could alter lipid distribution at the apical end is unclear. However, several studies showed that rhoptries are labile structures, which can discharge their contents upon stimulation by tannic acid or the carbohydrate stain, ruthenium red (10, 11, 29).

Several investigators (9–11, 29) have proposed that during invasion, material within the rhoptry is incorporated into the host membrane, facilitating PVM formation. Stewart *et al.* (10) localized membranous whorls in the rhoptry–microneme complex of the merozoite but not in trophozoites or immature schizonts. Our results support the view of a localized lipid concentration in the apical end of the merozoite and offer direct evidence for lipid injection into the host membrane during invasion.

The technical assistance of Cameron Cushing and Miguel Jurado is gratefully acknowledged. Research was supported by U.S. Public Health Service Grants P30 AM 34928, R01 AI 23457, R01 AI 21667, and R01 AI 24307.

1. Dvorak, J. A., Miller, L. H., Whitehouse, W. C. & Shiroishi, T. (1975) *Science* **187**, 748–749.
2. Aikawa, M., Miller, L. H., Johnson, J. & Rabbege, J. (1978) *J. Cell Biol.* **77**, 72–82.
3. Bannister, L. H., Butcher, G. A., Dennis, E. D. & Mitchell, G. H. (1975) *Parasitology* **71**, 483–491.
4. Vanderberg, J. P., Gupta, S. K., Schulman, S., Oppenheim, J. D. & Furthmayr, H. (1985) *Infect. Immun.* **47**, 201–210.
5. Mitchell, G. H., Hadley, T. J., McGinnis, M. H., Klotz, F. W. & Miller, L. H. (1986) *Blood* **67**, 1519–1521.
6. Perkins, M. E. (1984) *J. Exp. Med.* **160**, 788–798.
7. Friedman, M. J., Fukuda, M. & Laine, R. A. (1985) *Science* **228**, 75–77.
8. Okoge, V. C. & Bennet, V. (1985) *Science* **227**, 169–171.
9. Ladda, R., Aikawa, M. & Spinz, H. (1969) *J. Parasitol.* **55**, 633–644.
10. Stewart, M. J., Schulman, S. & Vanderberg, J. P. (1986) *Am. J. Trop. Med. Hyg.* **35**, 37–44.
11. Stewart, M. J., Schulman, S. & Vanderberg, J. P. (1985) *J. Protozool.* **32**, 280–283.
12. Holder, A. A. & Freeman, R. R. (1982) *J. Exp. Med.* **156**, 1528–1538.
13. Perlmann, H., Berzin, K., Wahlgren, M., Carlsson, J., Bjoerkman, A., Pattarroyo, M. E. & Perlmann, P. (1984) *J. Exp. Med.* **159**, 1686–1704.
14. McLaren, D. J., Bannister, L. H., Trigg, P. I. & Butcher, G. A. (1979) *Parasitology* **79**, 125–139.
15. Aikawa, M., Miller, L. H., Rabbege, J. R. & Epstein, N. (1981) *J. Cell Biol.* **91**, 55–62.
16. Wunderlich, F., Staubig, H. & Konigk, E. (1982) *J. Protozool.* **29**, 49–59.
17. Vial, H. J., Thuet, M. J. & Philippot, J. R. (1982) *J. Protozool.* **29**, 258–263.
18. Vial, H. J., Philippot, J. R. & Wallach, D. F. H. (1984) *Mol. Biochem. Parasitol.* **13**, 53–65.
19. Trager, W. & Jensen, J. B. (1976) *Science* **193**, 673–675.
20. Nillni, E. A., Schmidt-Ullrich, R., Mikkelsen, R. B. & Wallach, D. F. H. (1985) *Mol. Biochem. Parasitol.* **17**, 219–238.
21. Folch, J., Lees, M. & Stanley, G. H. S. (1957) *J. Biol. Chem.* **226**, 497–509.
22. Brown, J., Whittle, H. C., Berzin, K., Howard, R. J., Marsh, K. & Sjoberg, K. (1986) *Clin. Exp. Immunol.* **63**, 135–140.
23. Schmidt-Ullrich, R., Brown, J., Whittle, H. & Lin, P. S. (1986) *J. Exp. Med.* **163**, 179–188.
24. Kozbor, D., Lagarde, A. E. & Roder, J. C. (1982) *Proc. Natl. Acad. Sci. USA* **79**, 6651–6655.
25. Langreth, S. (1977) *Bull. WHO* **55**, 171–178.
26. Van Dyke, K., Trusch, M. A., Wilson, M. E. & Stealey, P. C. (1977) *Bull. WHO* **55**, 253–265.
27. Lantz, C. H. & Van Dyke, K. (1972) *Biochem. Pharmacol.* **21**, 891–894.
28. Haneard, R. J., Lyon, J. A., Diggs, C. L., Haynes, D., Leech, J. H., Barnwell, J. W., Aley, S. B., Aikawa, M. & Miller, L. H. (1984) *Mol. Biochem. Parasitol.* **13**, 53–65.
29. Bannister, L. H., Butcher, G. A. & Mitchell, G. H. (1977) *Bull. WHO* **55**, 163–169.